L. Cheng
Department of Mechanical Engineering, Laval University, Québec, Québec G1K 7P4, Canada

Vibroacoustic Modeling of Mechanically Coupled Structures: Artificial Spring Technique Applied to Light and Heavy Mediums

This article deals with the modeling of vibrating structures immersed in both light and heavy fluids, and possible applications to noise control problems and industrial vessels containing fluids. A theoretical approach, using artificial spring systems to characterize the mechanical coupling between substructures, is extended to include fluid loading. A structure consisting of a plate-ended cylindrical shell and its enclosed acoustic cavity is analyzed. After a brief description of the proposed technique, a number of numerical results are presented. The analysis addresses the following specific issues: the coupling between the plate and the shell; the coupling between the structure and the enclosure; the possibilities and difficulties regarding internal soundproofing through modifications of the joint connections; and the effects of fluid loading on the vibration of the structure. © *1996 John Wiley & Sons, Inc.*

INTRODUCTION

Structures submerged in a fluid medium have wide applications in the industrial market. Due to the interaction between the vibrating structure and the fluid motion, the majority of such problems require an analysis to take into consideration the mutual coupling between the structure and the fluid. Typical examples of such situations are structures surrounded by a heavy fluid and industrial vessels containing a liquid. A similar situation arises in cases involving internal acoustic radiation produced by a vibrating structure. In such cases, the structural vibration and the pressure field inside the enclosure form a complicated coupled system. This coupling process is illustrated schematically in Fig. 1, where it is shown that three physical mechanisms, in the form of structural vibration, acoustic radiation, and fluid–structure interaction, have to be mutually accounted for. This obviously requires an appropriate modeling procedure.

The so-called artificial spring technique, recently developed by Cheng and Nicolas (1992a) and Yuan and Dickinson (1992), would seem to be an ideal tool for handling such problems. The technique was initially developed to study the free vibrations of mechanical coupled structures consisting of a number of components or substructures. Cheng and Nicolas (1992a) studied a circular cylindrical shell closed at one end by a flexible plate, using artificial springs at the shell–

Received January 13, 1995; Accepted November 14, 1995.
Shock and Vibration, Vol. 3, No. 3, pp. 193–200 (1996)

CCC 1070-9622/96/030193-08

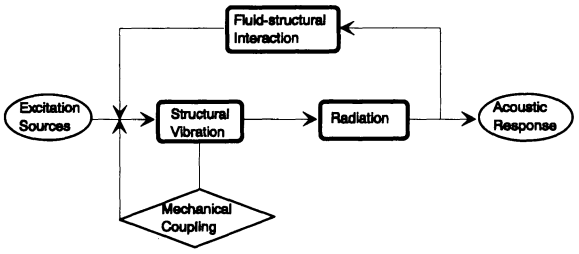

FIGURE 1 Schematic diagram of the coupling process.

plate junction to simulate the mechanical coupling. At almost the same time, Yuan and Dickinson (1992) published an article dealing with straight and curved beams using the same idea. More recently, the technique has been applied to much more complex systems to assess the method from the point of view of vibration analysis without any fluid coupling (Missaoui et al., 1996; Yuan and Dickinson, 1994). It was shown that the technique was quite convenient and efficient in handling the mechanical coupling problem. It was found that, when using the Rayleigh–Ritz method for analyzing such systems, the admissible functions should satisfy not only the geometrical boundary conditions but also the continuity with adjoining components, which is a quite difficult task. In the proposed approach, this continuity was automatically assured by permitting the stiffness of the artificial springs to become very large compared to the stiffness of the system. Moreover, a suitable combination of spring stiffnesses makes it possible to simulate a large variety of intermediate coupling cases.

The present article discusses the extension of the technique to vibroacoustic problems. As is well known, some of the most common methods for joined structures, such as the receptance method (Amizi, 1988) and the transfer matrix method (Irie, 1984), are restricted to vibration analysis. These methods soon become cumbersome when one wishes to deal with radiation problems where the structure is coupled to the acoustic medium. Taking the plate-ended cylindrical shell as an example, we propose to extend the previous free vibration analysis to include the fluid loading from the enclosed cylindrical cavity. Both light and heavy fluids are considered. It is shown that the proposed modeling takes into account fluid–structure coupling. Numerical results are then presented to highlight the physical phenomena and provide guidelines for soundproofing.

MODELING AND ANALYSIS

Model of Closed Cylindrical Shell

The model was initially established to study the cabin noise of an airplane. Preliminary tests on the airplane identified significant sources of mechanical excitation transmitted from the engines, which were attached directly to the aircraft body near the rear pressure bulkhead. Therefore, the aircraft fuselage and the bulkhead are considered to be the two main components affecting the cabin noise. The model investigated consists of a finite circular cylindrical shell closed at its left end ($x = 0$) by a flexible plate and at its right end ($x = L$) by a rigid cap (Fig. 2). Both the shell and the plate are assumed to be thin homogeneous structures. The whole structure is assumed to be supported initially by a shear diaphragm at each end. The excitations are unit point harmonic loads applied at arbitrary locations either on the shell or on the plate.

Principle of Artificial Spring Technique

The artificial spring technique was fully explained by Cheng and Nicolas (1992a) and Yuan and Dickinson (1992). Readers are referred to the previous works for more details. We recall very briefly the principle behind the technique.

The classical Rayleigh–Ritz method is a powerful approach for analyzing the free vibrations of structures. However, to ensure good simulation results, the trial functions must at least satisfy the geometrical boundary conditions associated with the translation and rotation (Meirovitch, 1969). For complex structures, the so-called geometrical boundaries require the continuity between all substructures at the various junctions. This requirement makes the choice of the trial functions very difficult. The use of artificial spring

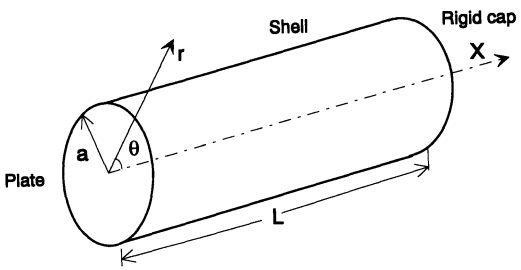

FIGURE 2 Schematic diagram of the structure under investigation.

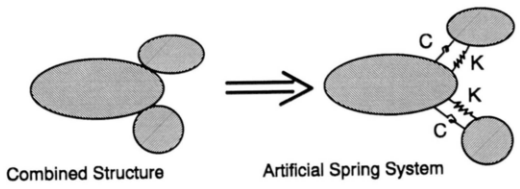

FIGURE 3 Schematic representation of the coupling modeling using the artificial spring system.

systems at a junction allows one to overcome this difficulty. As shown in Fig. 3, a virtual set of distributed spring systems is introduced at each junction and for every permitted degree of freedom. By allowing the spring stiffness to become very high compared to the stiffness of the components, one can approximate a rigid connection. The use of springs replaces the geometrical continuity conditions by corresponding dynamic conditions involving the strain energy of the springs. As a result, the choice of the trial functions is simplified, because the latter only have to satisfy the geometrical boundary conditions at the nonconnected regions. Thus, the classical Rayleigh–Ritz method can be applied, considering the spring system as a dynamic element of the whole system. Following the principles outlined above, we give a brief description of the mathematical formulation of the problem. Full details can be found in the studies of Cheng and Nicolas (1992a) and Cheng (1994).

Analysis of Structure

The whole structure is divided into two components connected by a set of artificial springs. Translational and rotational springs, having, respectively, distributed stiffnesses K and C, are added between the shell and the plate along the junction edge. All spring constants are defined in the appropriate units of stiffness per unit length along the contour and are assumed to be constant.

The shell displacements u, v, and w are then decomposed in terms of the eigenfunctions of a shear diaphragm supported shell as:

$$\begin{Bmatrix} u \\ v \\ w \end{Bmatrix} = \sum_{\alpha=0}^{1} \sum_{n=0}^{\infty} \sum_{m=1}^{\infty} \sum_{j=1}^{3} A_{nmj}^{\alpha}(t) \prod_{nmj}^{\alpha}(\alpha, n, m, j), \tag{1}$$

where $\prod_{nmj}^{\alpha}$ is the eigenvector of the shear diaphragm shell with n and m representing, respectively, the circumferential and the longitudinal order, α indicating symmetric ($\alpha = 1$) or antisymmetric ($\alpha = 0$) mode, and j the type of mode (bending, twisting, extension–compression); the $A_{nmj}^{\alpha}(t)$ are the coefficients to be determined.

The flexural displacement of the plate w_p is decomposed on a polynomial basis:

$$w_p = \sum_{\alpha=0}^{1} \sum_{n=0}^{\infty} \sum_{m_p=0}^{\infty} B_{nm_p}^{\alpha}(t) \Lambda_{nm_p}^{\alpha}(\alpha, n, m_p),$$

$$\Lambda_{nm_p}^{\alpha}(\alpha, n, m_p) = \sin(n\theta + \alpha\pi/2)(r/a)^{m_p}, \tag{2}$$

where n, m_p, and α are, respectively, the circumferential order, the radial order, and the symmetric index; a is the radius of the plate; and the $B_{nmj_p}^{\alpha}(t)$ are the coefficients to be determined.

We then calculate the Hamiltonian H of the whole system.

$$H = \int_{t_0}^{t_1} (T_c - E_c + T_p - E_p - E_k + E_F)dt, \tag{3}$$

where t_0 and t_1 are arbitrary times; T_c and T_p and E_c and E_p are respectively the kinetic and potential energies of the cylindrical shell and the plate; E_k is the potential energy stored in the springs; and E_F is the work done by the driving forces, including fluid loading from the cavity.

The governing equations of the plate-ended shell are obtained by applying the variational principle to find the extremum of the Hamiltonian over the subspace of the previous trial displacement functions satisfying:

$$\delta H = 0. \tag{4}$$

Analysis of Cavity

By neglecting the influence of the outer fluid medium, the sound pressure inside the cavity P_c can be calculated by means of the Green's function G, with Neumann boundary conditions with

$$P_c = \int_{S_1} G\rho\omega^2 w dS_1 - \int_{S_2} G\rho\omega^2 w_p dS_2, \tag{5}$$

where S_1, S_2, ρ, and ω are, respectively, the shell and plate area and the fluid density and the frequency. The Green's function G and the pressure P_c are then expanded in terms of the acoustic modes of the hard-walled cavity Φ_N leading to

$$P_c = \rho c^2 \sum_{N=1}^{\infty} P_N / M_N, \tag{6}$$

$$M_N \delta_{NM} = \frac{1}{V} \int_V \Phi_N \cdot \Phi_M dV, \tag{7}$$

with P_N the coefficients to be determined, V the volume occupied by the cavity, and δ_{NM} the Kronecker delta function. The second expression reflects the orthogonality of the acoustic modes.

Inserting Eq. (6) into (5) and using the orthogonality property of the acoustic modes yields a set of ordinary differential equations describing the internal sound pressure and the coupling with the structural vibrations.

Coupling Equations

The previous equations can be summarized as follows:

$$[\mathbf{S}] \begin{Bmatrix} A^{\alpha}_{nmj} \\ B^{\alpha}_{nm,} \\ P_N \end{Bmatrix} = \begin{Bmatrix} F^{\alpha(\text{shell})}_{nmj} \\ F^{\alpha(\text{plate})}_{nm,} \\ 0 \end{Bmatrix} \tag{8}$$

where [**S**] is the system matrix and the three right-hand side terms are the generalized forces corresponding to the decomposed terms of the shell and the plate.

The coupling equations, Eq. (8), can then be resolved for the complete fluid–structure system.

NUMERICAL RESULTS, DISCUSSION AND CONCLUSIONS

Numerical results are presented for the average sound pressure level inside the cavity and for the quadratic velocity of the shell and the end plate. As far as shell response is concerned, only radial velocities are considered. The quadratic velocity is represented in terms of decibels referenced to $5 * 10^{-8}$ m/s. The shell and the plate are assumed to have the same material properties as aluminum (Young's modulus, $7 * 10^{10}$ N/m^2; density, $2.7 * 10^3$ kg/m^3; and Poisson's coefficient, 0.3). The dimensions of the shell are $L = 1.2$ m and $a = 0.3$ m. The thicknesses of the shell and the end plate were chosen to be the same and are equal to 3 mm. The input load, consisting of a unit point force, acted at fixed locations on the shell surface ($x = 0.35$ m) or the end-plate surface ($r = 0.2$ m). A damping factor of 1% was used for both the structure and the cavity. Two nondimensional stiffness parameters are defined as: $\hat{K} = Ka^3/D_p$, $C = Ca/D_p$ where D_p is the flexural rigidity of the plate.

Figure 4 illustrates the three types of modes for the combined structure, using the so-called frequency parameter Ω_i^*, defined as the ratio between the natural frequency of the structure and the ring frequency of the shell. The three types are referred to respectively as plate-controlled, shell-controlled, and coupled modes. It should be noted that the resulting motions are dominated by different components depending on the mode.

One of the merits of the technique is its ability to use modal information on each substructure to accelerate the convergence speed compared with other classical numerical approaches (Cheng and Nicolas, 1992a). In the case under study, the reason is believed to be twofold: for the shell, a "physical" base is used, in nature quite similar to the real structure (as far as the shell portion is concerned); for the plate, the boundary is uniform and homogeneous, although the expansion series is less physical. As pointed out by Pierre et al. (1987), irregularities present in structures may be a key factor in slowing down the convergence of the Rayleigh–Ritz procedure. In our case however, the shell–plate connection is uniform and symmetric, so this problem did not present itself.

Figures 5 and 6 illustrate the average quadratic velocities of the structure with the excitation force applied to the shell and plate surface, respectively. In the calculations, the plate is assumed to be rigidly attached to the shell with $\hat{K} = \hat{C} = 10^8$. When the shell excited directly (Fig. 5), one can clearly identify the presence of shell-controlled modes and some coupled modes in the spectrum of the shell response. However, no plate-controlled modes are noticeable in this shell response spectrum. It is in the spectrum of the plate that the plate-controlled modes, together with shell-controlled and coupled modes, appear. As far as the response of the plate is concerned, we notice a relatively low level at low frequencies. Figure 6 provides similar information except that the vibration is dominated by plate-controlled and coupled modes. Therefore, the coupling between the shell and the plate is generally weak at low frequencies. The vibration response of the substructure that is directly excited, is dominated by its own modes and coupled modes. Modes of every nature, that is to say plate-controlled, shell-controlled, and coupled modes, generally appear in the response spectrum of the substructure that is not directly excited. The shell–plate coupling becomes more notice-

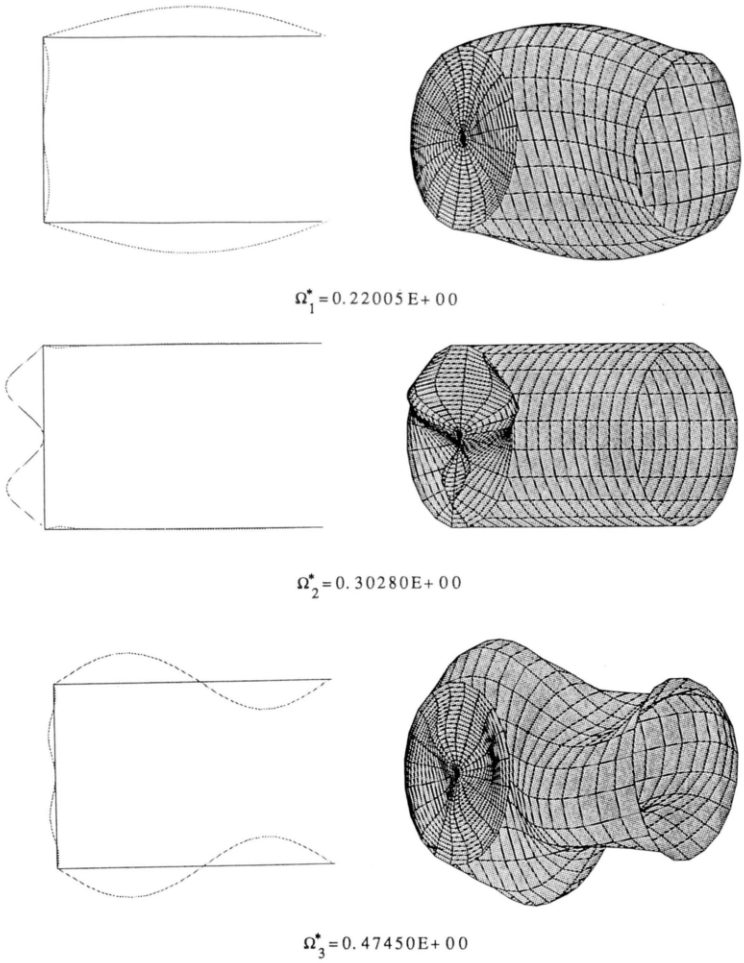

FIGURE 4 Three typical normal modes of the combined structure: (a) shell-controlled modes; (b) plate-controlled modes; (c) coupled modes.

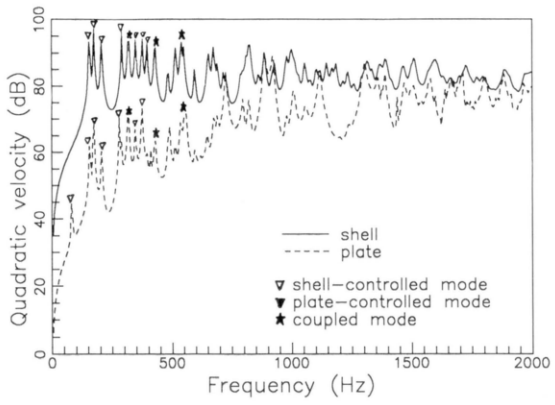

FIGURE 5 Quadratic velocity of the structure with the shell subjected to a unit point load.

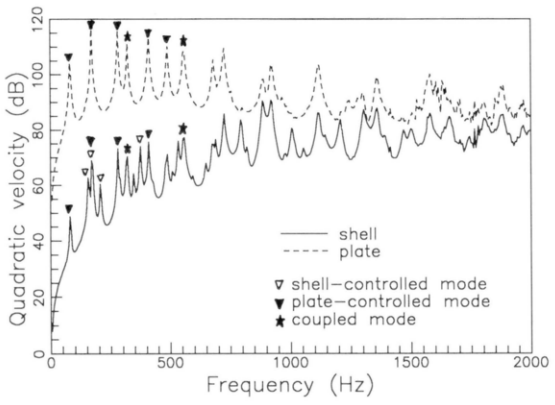

FIGURE 6 Quadratic velocity of the structure with the end plate subjected to a unit point load.

able at higher frequencies. To better illustrate the energy distribution between the shell and the plate, Fig. 5 and 6 are retreated. The quadratic velocity ratios between the shell and the plate in decibels are plotted in Fig. 7 for the two excitation cases used above. It shows that in both cases, the curves asymptotically approach the 0-dB level indicating an equal distribution.

Figure 8 presents the corresponding sound pressure levels inside the cavity when the driving force is applied either on the shell or the plate. It can be seen that cavity noise arises mainly from the directly excited substructure at low frequencies. The sound pressure level inside the cavity is much higher when the excitation is applied to the end plate. The reason for this is that the plate modes generally couple well with the cavity modes; whereas the shell modes, although participating actively in the overall structure response, do not couple efficiently with the acoustic ones in this frequency range. The observed phenomena can be easily explained by inspecting the dispersion relation of the shell, plate, and cavity. Consequently, from the soundproofing point of view, direct excitations on the plate should be avoided.

The previous analysis was made for a particular configuration in which the critical frequency is higher than the ring frequency of the shell. If the ring frequency is higher than the critical frequency, resulting either from an increase of the shell thickness or a decrease of the radius of the shell, the conclusion concerning the vibration energy distribution should still be valid. As a word of caution, however, the radius changes may affect the coupling between the structural modes and the cavity modes so that the internal acoustic field might be affected. Because different parameters are involved in this case, a detailed parameter analysis is considered to be beyond the scope of this study.

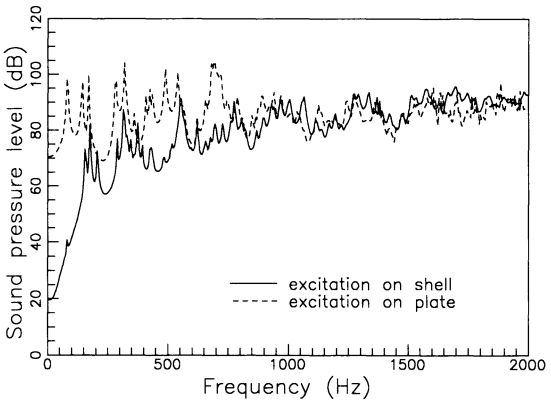

FIGURE 8 Average sound pressure levels inside the cavity generated by the motion of the structure with the shell and the end plate, respectively, subjected to a unit point load.

We will present a few numerical results also to illustrate the influence of the joint conditions between the shell and the plate on the generated cavity noise.

Figure 9 shows the effects of the translational spring constant K on sound pressure levels inside the cavity with the plate subjected to a driving force. The results are presented in one-third octave bands. It can be seen that in the absence of the translational coupling, the structure radiates much less sound over a very large frequency range except at very low frequencies. This observation is consistent with the one made in a previous work (Cheng and Nicolas, 1992b) where the sound radiation to a cylindrical hard-walled cavity by a single plate with various boundary condi-

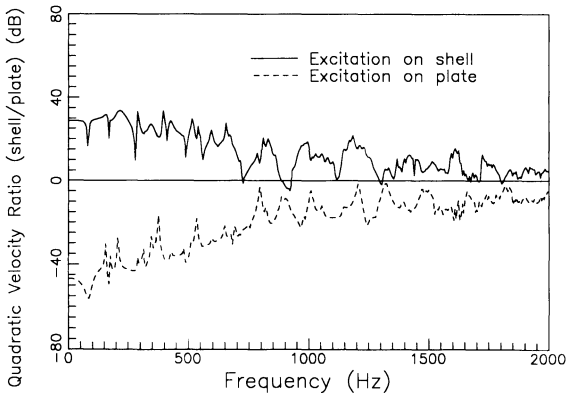

FIGURE 7 Ratio between the quadratic velocity of the shell to that of the plate.

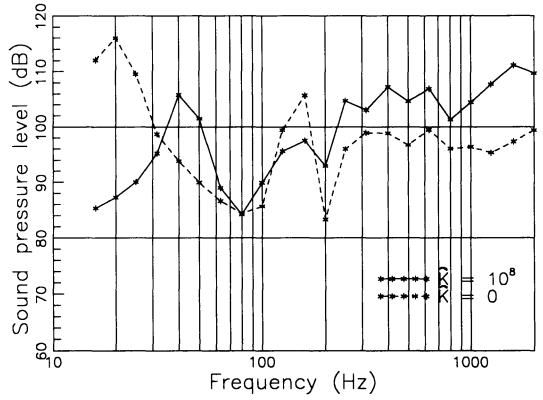

FIGURE 9 Average sound pressure level inside the cavity in one-third octave bands with two limiting shell–plate joint conditions in translation.

tions was investigated. Similar phenomena were observed in previous studies regarding the translational support of the plate. A detailed analysis showed that relaxing the translational support of the plate significantly reduces the radiation efficiency of the plate modes and consequently, the generated noise. Figure 9 shows that the fact that the cylindrical wall is a flexural envelope does not fundamentally change this trend. In addition, reducing K reduces the plate–shell coupling via translation, so that the contribution of the shell radiation, although small in the present case, is also reduced.

Figure 10 illustrates the effects of the rotational spring constant C, coupling the plate with the shell via a rotation along the edge. The noise levels are much less sensitive to changes in the rotational coupling C than those in K. Although small differences existed at low frequencies, the noise inside the cavity is not very sensitive to rotational coupling up to 700 Hz. Above 1,000 Hz, the noise level is reduced appreciably by reducing the rotational coupling. However, with a hard-walled cylindrical cavity, Cheng and Nicolas (1992b) showed that no such trend was observed when softening the rotational fixation of the end plate; and it was shown that the radiation properties of the plate cannot be systematically improved by changing the rotational supports, unlike the translational case. It is therefore felt that the noise reduction obtained in the present case is due to the fact that by relaxing the rotational coupling, vibration levels of the shell are reduced and consequently, so is its sound radiation. A more elaborate investigation shows that the shell is indeed coupled to the plate, mainly through rotation. Similar investigations have been performed with excitation loads applied to the shell surface. However, it appears that the changes in the coupling conditions in this case do not indicate general trends as in the case of plate excitations.

From Fig. 9 and 10, we drew the following conclusions: when the excitations are applied to the shell, changing the joint conditions does not provide any systematic improvement as regards the radiated sound field inside the cavity. However, when the end plate is directly excited, reducing the stiffness of the joint between the shell and the plate proves to be a good means to reduce cavity noise. Two different mechanisms are involved: the reduction of the translational coupling along the longitudinal axis of the shell significantly reduces the radiation efficiency of the plate modes and softening the rotational coupling reduces the mechanical energy transferred to the shell. In both cases, cavity noise is reduced. However, a relaxation of the translational coupling seems to give better results in terms of a greater noise reduction over a broader frequency band.

The model is equally valid as a means of simulating a fluid enclosed in a cylindrical vessel with end caps. An example is presented to show the influence of the fluid density. Retaining the case of a unit point driving force, Fig. 11 and 12 show, respectively, the structural response to a harmonic input applied to the shell surface when the structure is filled with both light (air) and heavy (water) fluid. Several interesting points are worth mentioning. The first point is illustrated in Fig. 11 which compares the vibration level of the structure containing air with the case when the fluid is absent. It shows clearly that the presence of the air, which is considered to be a light fluid, has very little influence on the dynamic behavior of the structure. At a few resonances, the vibra-

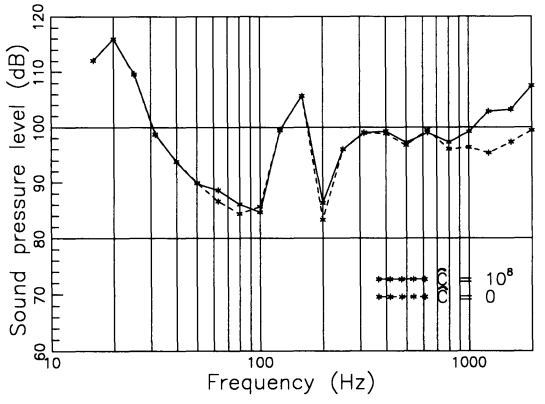

FIGURE 10 Average sound pressure level inside the cavity in one-third octave bands with two limiting shell–plate joint conditions in rotation.

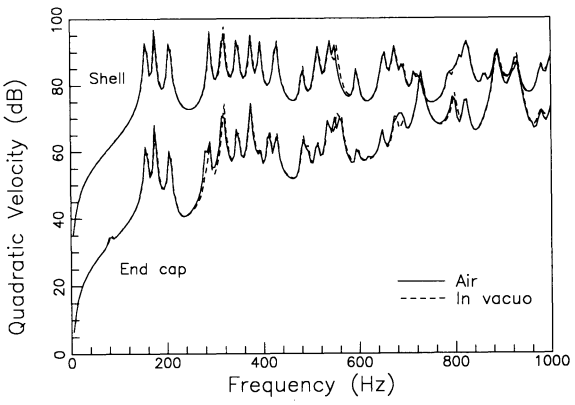

FIGURE 11 Quadratic velocity of the vessel in air and in vacuo.

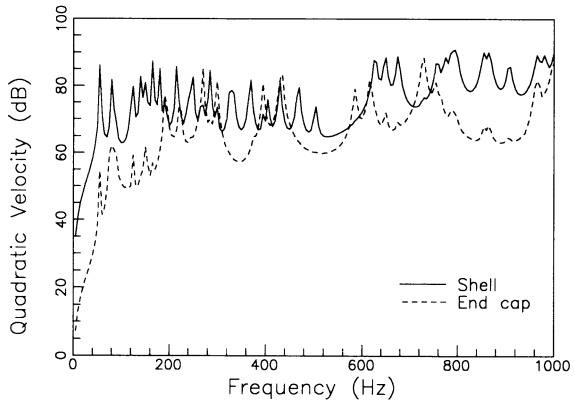

FIGURE 12 Quadratic velocity of the vessel containing water.

tion level of the structure seems to be slightly modified, indicating that the presence of the air, although light, has an influence in terms of mass, stiffness, and damping effect on the system. It can also be seen from Fig. 11 that the vibration level of the shell is much greater than that of the end cap. All the peaks emerging from the spectra are found to virtually coincide with the natural frequencies of the in vacuo structure, which clearly demonstrates that the structure–air coupling is extremely weak. The second point is that in the case of the structure containing water, Fig. 12 shows that all the previous peaks are shifted significantly toward the low frequencies, proving that the coupling between the structure and the water is important and that the fluid engenders significant mass effects on the structure. In addition, due to the presence of the water, the vibration level of the end cap is brought to a comparable level with that of the shell, which is the substructure being directly excited. This observation highlights the fact that the mechanical energy generated by the shell is transmitted to the end plate via the fluid. Consequently, the end cap is excited in a more significant manner. Lastly, by comparing Figs. 11 and 12, one can see that the presence of water in the enclosure reduces the vibration level of the shell and, generally, brings down the vibration level of the whole structure.

CONCLUDING REMARKS

The artificial spring technique was successfully applied to the vibroacoustic analysis of a closed cylindrical structure. The proposed formulation can be applied to cases where the structure is filled with either light or heavy fluids. Different examples were analyzed to illustrate the versatility of the approach. The method is simple to use when each subsystem is amenable to analysis using the Rayleigh–Ritz method. As a word of caution, it should be noted that the method can become cumbersome when the number of subsystems increases, resulting in a need for an increasing number of spring systems. Also, the speed of convergence can be significantly slowed down by the presence of strong discontinuities or the lack of suitable physical trial functions. These issues will be addressed more specifically in our future work.

REFERENCES

Amizi, S., 1988, "Free Vibration of Circular Plates with Elastic Edge Supports Using the Receptance Method," *Journal of Sound and Vibration*, Vol. 120, pp. 19–35.

Cheng, L., and Nicolas, J., 1992a, "Free Vibration Analysis of a Cylindrical Shell-Circular Plate System with General Coupling and Boundary Conditions," *Journal of Sound and Vibration*, Vol. 155, pp. 231–247.

Cheng, L., and Nicolas, J., 1992b, "Radiation of Sound into a Cylindrical Enclosure from a Point-Driven End Plate with General Boundary Conditions," *Journal of the Acoustics Society of America*, Vol. 91, pp. 1504–1513.

Cheng, L., 1994, "Fluid–Structure Coupling of a Plate-Ended Cylindrical Shell: Vibration and Internal Sound Field," *Journal of Sound and Vibration*, Vol. 174, pp. 641–654.

Irie, T., 1984, "Free Vibration of Joined Conical-Cylindrical Shells," *Journal of Sound and Vibration*, Vol. 95, pp. 31–39.

Meirovitch, L., 1969, *Analytical Methods in Vibrations*, Macmillan, New York.

Missaoui, J., Cheng, L., and Richard, M., 1994, "Free and Forced Vibration of a Cylindrical Shell with a Floor Partition," *Journal of Sound and Vibration*, Vol. 190, pp. 21–40.

Pierre, C., Tang, D. M., and Dowell, E. H., 1987, "Localized Vibrations of Disordered Multispan Beam: Theory and Experiment," *American Institute of Aeronautics and Astronautics Journal*, Vol. 25, pp. 1249–1257.

Yuan, J., and Dickinson, S. M., 1992, "On the Use of Artificial Springs in the Study of the Free Vibrations of Systems Comprised of Straight and Curved Beams," *Journal of Sound and Vibration*, Vol. 153, pp. 203–216.

Yuan, J., and Dickinson, S. M., 1994, "The Free Vibration of Circularly Cylindrical Shell and Plate Systems," *Journal of Sound and Vibration*, Vol. 175, pp. 241–263.